Neural responses to binocular in-phase and anti-phase stimuli

Bruno Richard[1], Daniel H. Baker[2]

[1]Department of Math and Computer Sciences, Rutgers University, Newark, New Jersey, USA
[2]Department of Psychology, University of York, York, UK

Abstract

VSS Abstract - Binocular vision fuses similar stimuli into a single percept, yet incompatible stimuli result in other experiences such as rivalry, lustre, and diplopia. We measured neural responses to binocular stimuli with different phase relationships, intending to understand them using contemporary binocular models. Steady-State Visually Evoked Potentials (SSVEPs) were recorded from 15 observers in response to monocular and binocular stimulation at 3Hz, using either on-off or counterphase flicker. Across the eyes, binocular stimuli could be (i) in spatial and temporal phase, (ii) in temporal phase but spatial antiphase, (iii) in spatial phase but temporal antiphase, or (iv) in spatial and temporal antiphase (for counterphase flicker this is identical to condition (i)). Responses to monocular on-off flicker showed peaks at the fundamental frequency (3Hz) and its harmonics (integer multiples of 3Hz). In contrast, counterphase flicker produced responses only at twice the flicker frequency (6Hz) and its harmonics. Binocular in-phase stimulation resulted in a similar pattern of responses, consistent with 'ocularity invariance' – the observation that binocular and monocular stimuli appear equal at high contrasts. Changing the phase relationship modulated the harmonics pattern in complex ways. On-off flicker in temporal antiphase reduced the fundamental response, but there was no such effect for counterphase flicker. We modelled the data using a progression of binocular combination algorithms that increased in complexity from a simple linear sum to a two-stage binocular gain control model with parallel monocular and binocular phase-selective channels (the Lustre model). The most complex model (lustre) outperformed all other models in capturing the variance of our SSVEP data, although simpler phase-insensitive models performed similarly well in most experimental conditions. Simpler models struggled to capture the response magnitude to counterphase stimuli. Our findings suggest that explaining neural responses to binocular stimuli with different phase relationships requires parallel monocular and phase-selective channels.

Introduction

The human visual system integrates input from both eyes to form a unified binocular representation of the world. Combining monocular inputs enhances sensitivity to the presented

stimuli, particularly when the contrast is low or near detection threshold (Baker et al., 2018; Campbell and Green, 1965; Meese et al., 2006). Contrast sensitivity can improve by a factor of $\sqrt{2}$ or more when stimuli are presented binocularly versus monocularly (Baker et al., 2018; Blake and Wilson, 2011; Campbell and Green, 1965; Richard et al., 2018). Notably, the visual system also attempts to combine inputs even when the stimuli presented to each eye are markedly different (i.e., incompatible). In such cases, observers may perceive binocular rivalry (Blake, 1989; Wilson, 2003), diplopia, or visual lustre (Georgeson et al., 2016). Despite differences in perceptual outcomes, computationally, the underlying processes of binocular combination for compatible and incompatible inputs appear similar (Baker et al., 2007a; Legge, 1984). Human behavioural responses to compatible and incompatible stimuli can be effectively explained by a single psychophysical model that involves nonlinear transduction, followed by summation across monocular and binocular phase-selective channels (Baker et al., 2007a; Baker and Meese, 2007). Here we explore if the integrative processes defined over multiple behavioural tasks are also reflected at the neural level.

It has long been known that stimuli presented binocularly are summed across the eyes. In contrast detection tasks, where stimulus contrast is low, binocular presentation increases sensitivity by approximately $\sqrt{2}$ (Campbell and Green, 1965). This implies that observers require roughly 1.4 times more contrast to detect a monocular stimulus than a binocular one. The binocular improvement in sensitivity is consistent with a non-linearity operating before the signals from the two eyes (C_L and C_R) are combined (Legge, 1984):

$$R_B = C_L^m + C_R^m. \tag{1}$$

Here, the exponent m determines the degree of summation. When $m = 1$, summation is linear, yielding a doubling of sensitivity. When $m = 2$, summation is reduced to $\sqrt{2}$. Several studies have reported summation ratios over $\sqrt{2}$ with some approaching 1.8 (Meese et al., 2006; Simmons, 2005; Simmons and Kingdom, 1998). A recent meta-analysis of 65 studies (N = 716) found an average binocular summation ratio of 1.5 (Baker et al., 2018). This work highlighted the challenges in accurately describing the binocular summation process (e.g., m) as individual variability and methodological differences can greatly impact binocular summation.

The contrast of stimuli, for example, is crucial in measuring binocular summation. Binocular summation can be very large when stimulus contrast is low; however, the binocular advantage is seldom observed in tasks that involve higher contrasts. In contrast discrimination tasks, where observers judge the contrast difference between otherwise identical stimuli, binocular presentation no longer confers a benefit in sensitivity (Legge, 1984; Maehara and Goryo, 2005; Meese et al., 2006): discrimination thresholds are identical whether stimuli are shown to one eye or both. This does not mean binocular signals are not combined at higher contrasts (Meese et al., 2006; Meese and Baker, 2011). Instead, the advantage of summation is counteracted by normalization mechanisms that maintain consistency across viewing conditions (referred to as 'ocularity invariance'). In contrast gain control models of early vision, normalization can stem from interocular and self-suppressive signals (Meese et al., 2006):

$$R_B = \frac{C_L^m}{S + C_L + C_R} + \frac{C_R^m}{S + C_R + C_L}. \tag{2}$$

When both eyes are stimulated, the suppressive terms on the denominators offset the enhanced excitatory signals, nullifying the binocular advantage.

A similar pattern of results is observed in neural measurements of binocular summation. In fMRI recordings, neural responses are significantly larger for binocular than monocular responses when stimulus contrast is low (Moradi and Heeger, 2009). At higher contrasts, observers no longer show the binocular advantage. These findings were well-explained by a model including interocular suppression and binocular contrast normalization, an identical mechanism to that used to explain behavioural data. The equivalency in binocular summation between psychophysics and neuroimaging findings means that both data types can be used to constrain binocular summation models. We, for example, have previously demonstrated that a popular model of binocular summation could be easily adapted to capture Steady-State Visually Evoked Potentials (SSVEPs) to monocular and binocular stimuli when one eye was occluded by a neutral density filter (Richard et al., 2018). Placing a neutral density filter in front of one eye darkens its input, reducing the amplitude and altering the phase of SSVEPs to stimuli presented to the filtered eye. Steady-State response amplitudes and phases to stimuli presented through different neutral density filter strengths were well described by a model that first used a biophysically plausible temporal filter on the input stimuli, followed by self and interocular suppression, and finally, binocular contrast normalization. This model also captures psychophysically measured binocular summation in the same group of observers. A comprehensive description of the processes involved in binocular summation should be able to explain behavioural and neuroimaging findings under various experimental conditions of binocular summation.

Many studies have worked towards the development of a comprehensive description of the process of binocular summation in human vision using a variety of psychophysical and neuroimaging data (Baker et al., 2008, 2007b; Ding et al., 2013; Ding and Sperling, 2006; Legge, 1984; Lygo et al., 2021; Maehara and Goryo, 2005; Richard et al., 2018). Developing these models is not an insignificant challenge; they must account for multiple components of early vision, including identifying relevant signals, defining how these signals might interact, what non-linearities are present, and most importantly, how they are combined. One such model that has proven very informative and capable of describing binocular summation under various experimental conditions is the two-stage contrast gain control model developed by Meese et al. (2006). The model captured detection and discrimination thresholds for monocular and binocular stimuli in addition to dichoptic stimuli, whereby the stimuli presented to both eyes are not identical, in a two-stage process. First, the input is rectified by an excitatory non-linearity ($m \approx 1.3$) and normalized by self and interocular suppression (see Equation 2). The binocular (e.g., combined) input undergoes a second contrast normalization before the decision stage,

$$R = \frac{R_B^p}{Z + R_B^q}, \tag{3}$$

where the excitatory exponent p allows for greater increase in sensitivity than would be seen by the excitatory non-linearity of the first stage (m in Equation 2) alone.

Subsequent iterations of the two-stage contrast gain control model added channels for

opposite contrast polarities (Baker and Meese, 2007), and monocular channels parallel the binocular summing channel (Georgeson et al., 2016). Polarity-specific channels were included to explain masking effects when the stimuli presented to each eye had opposing phase polarities (i.e., dichoptic presentation). The presentation of sinusoidal gratings with opposite polarities to each eye does not cancel them out: stimuli remain detectable and the two inputs sum, albeit weakly (Bacon, 1976; Baker and Meese, 2007; Simmons, 2005). Parallel monocular channels were added to account for adaptation after-effects that suggest monocular signals may be preserved and available for perception following binocular summation (Blake et al., 1981; Moulden, 1980). While the possibility of monocular channels had been considered (Legge, 1984), many assumed that only the binocularly summed signal contributed to perception. In a comprehensive study of binocular contrast perception, Georgeson et al. (2016) developed a specific experimental condition to assess the involvement of monocular channels. They devised a discrimination task where the target interval presented a contrast increment to one eye (e.g., 10% pedestal + 2%) and a contrast decrement to the other (e.g., 10% pedestal - 2%). If the only available signal is a binocularly summed one, the task would be nearly impossible to complete; the target interval would be perceptually identical to the pedestal-only interval. However, observers were able to complete the task. The two-stage contrast gain control model with parallel monocular channels was the only model able to capture observer thresholds from all experimental conditions, including the binocular increment and decrement condition.

The current architecture of the two-stage contrast gain control model has been rigorously evaluated on psychophysical data, providing a solid foundation for our understanding of binocular combination (Baker and Meese, 2007; Georgeson et al., 2016; Meese et al., 2006). While previous studies have utilized the two-stage contrast gain control model on neuroimaging data (Lygo et al., 2021; Richard et al., 2018), they only included experimental conditions where the phases of the sinusoidal gratings presented to each eye were identical. To accurately assess the current architecture of the two-stage contrast gain control model, neuroimaging data for binocular presentation of stimuli in opposite phase polarity are required. Here, we recorded SSVEPs to monocular and binocular stimuli with different spatial and temporal phase relationships to obtain the data needed to evaluate the two-stage contrast gain control model. By progressively increasing the complexity of the model, we demonstrate that many mechanisms of binocular combination, such as monocular non-linearities, interocular interactions, and parallel monocular channels, are required to explain neural responses to our set of experimental conditions. Thus, the two-stage contrast gain control model remains a powerful and flexible descriptor of the architecture of binocular combination for data collected across many experimental conditions and modalities.

Methods

Participants

Fifteen observers (including both authors: BR and DHB) with normal or corrected to normal visual acuity and binocular vision participated in our study. Written informed consent was obtained from all participants, and experimental procedures were approved by the ethics

committee of the Department of Psychology at the University of York.

Apparatus

All stimuli were presented using a gamma-corrected ViewPixx 3D display (VPixx Technologies, Canada) driven by a Mac Pro. Binocular separation with minimal crosstalk was achieved by synchronizing the display's refresh rate with the toggling of a pair of Nvidia stereo shutter goggles using an infrared signal. The monitor refresh rate was set to 120 Hz; each eye updated at 60 Hz (every 16.67 msec). The display resolution was set to 1920 X 1080 pixels. A single pixel subtended 0.027^o of visual angle (1.63 arc min) when viewed from 57 cm. The mean luminance of the display viewed through the shutter goggles was 26 cd/m^2.

EEG signals were recorded from 64 electrodes distributed across the scalp according to the 10/20 EEG system (Chatrian et al., 1985) in a WaveGuard cap (ANT Neuro, Netherlands). We monitored eye blinks with an electrooculogram consisting of bipolar electrodes placed above the eyebrow and the cheek on the left side of the participant's face. Stimulus-contingent triggers were sent from the ViewPixx display to the amplifier using a parallel cable. Signals were amplified and digitized using a PC with the ASAlab software (ANT Neuro, Netherlands). All EEG data were imported into MATLAB (Mathworks, MA, USA) using components of the *EEGlab* toolbox (Delorme and Makeig, 2004) and then exported for subsequent offline analysis using R.

Stimulus Creation

Observer SSVEPs were measured with a single horizontal sinusoidal grating that subtended 15° of visual angle on the retina with a spatial frequency of 3 cycles/^{o} of visual angle (Figure 1A). Our experimental conditions modulated the interocular spatial phase of stimuli (Figure 1A). Under binocular viewing, the sinusoidal gratings could be presented in spatial phase or spatial anti-phase. When stimuli were presented in spatial phase, the aligned sinusoidal gratings were identical in both eyes ($\Delta\phi = 0$). The spatial anti-phase condition phase-shifted one of the sinusoidal gratings by 180° ($\Delta\phi = \pi$). Stimuli were also modulated in their oscillatory pattern, which could be On/Off or counterphase flicker at a frequency of 3Hz (Figure 1B). Under On/Off contrast flicker, the relative contrast of the gratings began at 0%, increased smoothly to 100% of the nominal maximum (100% Michelson contrast), and then returned to 0% over 333 ms (i.e., one cycle). On/Off flicker will generate SSVEPs at the fundamental frequency (3Hz) and its integer harmonics (2F, 3F, 4F, see Figure 1C). Counterphase flicker reversed the phase of the gratings at a frequency of 3Hz. The contrast of the grating began at the relative maximum (100%), gradually decreased in contrast to 0% of the relative maximum, and then increased again to 100% but in the opposite phase polarity. Unlike On/Off flicker, counterphase flicker generates two nearly identical transients per cycle and thus does not produce SSVEPs at the fundamental frequency (3Hz) but only its even harmonics (Wade and Baker, 2025).

To aid with binocular fusion, stimuli were surrounded by a static binocular texture presented beyond the central 19° stimulus aperture. These textures were constructed by first low-pass filtering a white (amplitude $\propto 1/f^0$) noise pattern, dichotomizing its output into a

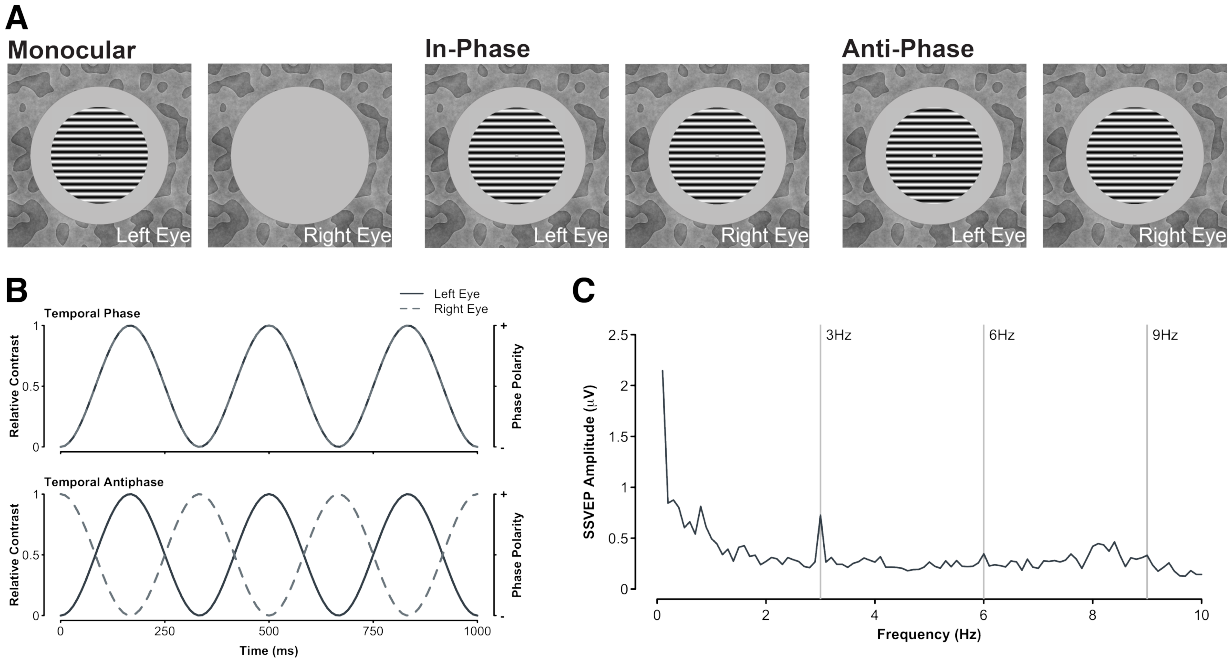

Figure 1: **A**. The spatial configuration of stimuli presented to observers in our experiment. Monocular conditions presented the sinusoidal grating to the left or right eye of observers (counterbalanced) while the other eye was presented with a gray screen set to mean luminance. Binocular conditions could be shown with stimuli in spatial phase, whereby the phase of both sinusoidal gratings was identical, or in spatial anti-phase, where the phase of the sinusoidal gratings presented to each eye was opposite. The background texture did not change throughout the trial to aid with binocular fusion. **B**. The temporal configuration of our stimuli. To generate SSVEPs, stimuli were contrast modulated in two ways: on/off (left Y axis) or counterphase (right Y axis). The oscillatory pattern could also be in phase (upper plot), where both stimuli were modulated in the same manner, or in counterphase (lower plot), where as one stimulus increased in contrast, the other decreased in contrast (or increased in opposite polarity). **C**. Example SSVEPs generated under binocular spatial and temporal in-phase viewing of stimuli for one observer, with an average of four electrodes (*Oz*, *POz*, *O1*, *O2*) and 12 repetitions.

binary image and taking its phase spectrum. A second flat (amplitude $\propto 1/f^0$) was adjusted by multiplying each spatial frequency's amplitude coefficient by f^{-1} to generate a pink amplitude spectrum (Hansen and Hess, 2006; Tadmor and Tolhurst, 1994). The pink amplitude spectrum and the phase spectrum of the binary image were rendered in the spatial domain by taking the inverse Fourier transform, resulting in the pattern shown in Figure 1A.

Procedures

Steady-State Visually Evoked Potentials (SSVEPs) were recorded with monocular and binocular stimulation using either on-off or counterphase flicker at 3Hz. Across the eyes, binocular stimuli could be in spatial and temporal phases, in temporal phase but spatial anti-phase, in spatial phase but temporal anti-phase, or spatial and temporal anti-phase (on-off flicker only). Stimuli presented in spatial and temporal anti-phase under counterphase flicker are identical to stimuli presented in spatial and temporal phase (and so we did not duplicate this condition). Thus, this experiment was comprised of a total of nine conditions - two monocular and seven binocular - which were each repeated 12 times for a total of 108 trials. Stimulus presentation was separated into four experimental blocks, each containing 27 trials. A trial lasted 15 seconds; a grating stimulus flickered onscreen for 11 seconds, followed by a screen with its central 19° set to mean luminance for 4 seconds. Participants completed all 27 trials of an experimental block in a single sequence (6.75 minutes) and were given breaks between experimental blocks. The trial order was pseudo-randomized on each block. Participants did not receive explicit task instructions other than to fixate the marker in the center of the display and blink only during the blank period between stimulus presentations.

SSVEP Analysis

We used whole-head average referencing to normalize each electrode to the mean signal of all 64 electrodes (for each sample point). The EEG waveforms were Fourier transformed at each electrode for a 10-second window, beginning one second after the stimulus onset to avoid onset transients. The Fourier spectra were coherently averaged (i.e., retaining the phase information) across four occipital electrodes (*Oz*, *POz*, *O1* and *O2*) and trial repetitions (see Figure 1C). We then calculated signal-to-noise ratios (SNRs) by dividing the absolute amplitude in the signal bin (e.g., 3 Hz) by the mean of the absolute value of the ten adjacent bins ($\pm$0.5 Hz in steps of 0.1 Hz). Given that distributions of SNRs are inherently skewed, the median SNR was taken across all participants; the median is a more robust descriptor of central tendency in skewed distributions.

Results

Figure 2 shows the cross-participant median SNR spectra for all experimental conditions. Responses for all On/Off flicker experimental conditions generated peaks at the fundamental frequency (3Hz) and its harmonics (integer multiples of 3Hz). Similarly, counterphase flicker produced responses at twice the flicker frequency (6 Hz) and its harmonics. We assessed differences in SNR magnitude across experimental conditions via a permutation test. A per-

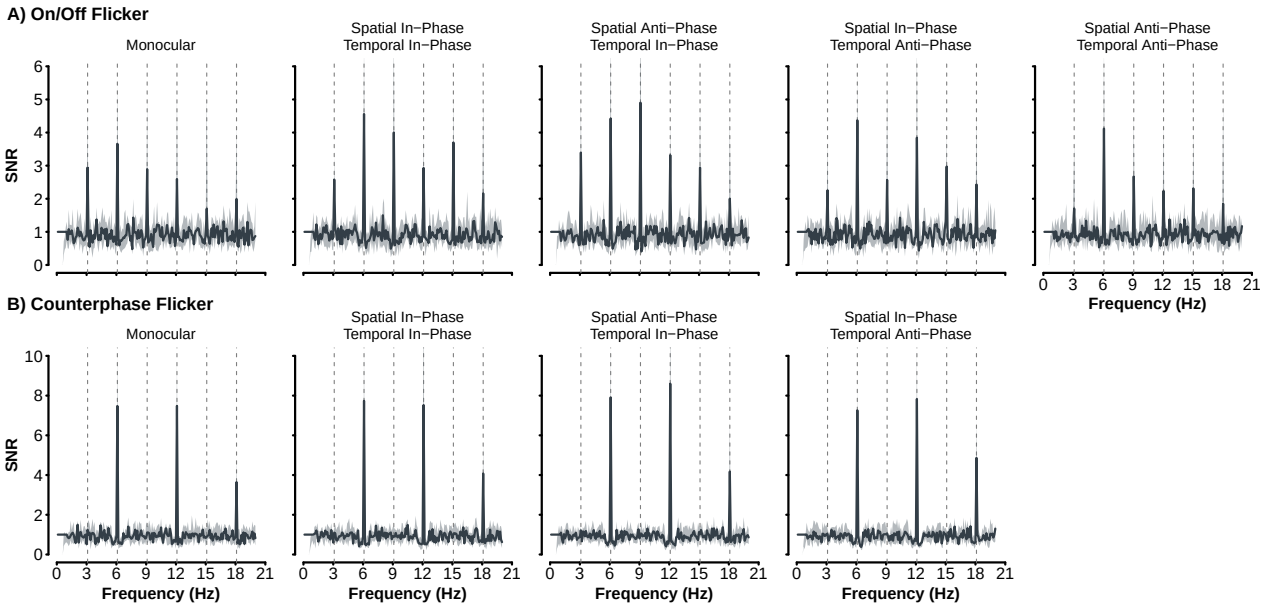

Figure 2: Cross-participant median SNRs for frequencies up to 20Hz. SNRs generated by On/Off flicker are shown in the top row (A), while those generated by counterphase flicker are shown in the bottom row (B). The light gray area represents 95% bootstrap confidence intervals that were calculated by resampling (with replacement) participant SNRs 2000 times.

mutation test allows for a non-parametric comparison of a statistic between two experimental conditions. We first take the median difference between two experimental conditions (i.e., the observed difference). A null distribution is then constructed by combining SNR values from both experimental conditions, and randomly sampled without replacement to create two groups of sizes identical to their original, but with values that are not associated with a particular experimental condition. The median difference of the randomly sampled SNRs is then taken. This process is repeated multiple times (e.g., $N = 2000$) to build a distribution of median differences with no association of experimental condition (i.e., a null-hypothesis distribution). The observed median difference is then compared to this distribution, and the proportion of scores greater (or less) than the observed difference represents the p value associated with the test. When comparing SNRs at the fundamental frequency (3Hz) for On/Off flicker, we find no statistically significant difference in median SNR magnitude between experimental conditions where stimuli were presented in temporal phase (see Figure 3). Monocular and binocular presentation for stimuli presented in temporal phase resulted in a similar response pattern under both On/Off and counterphase flicker modulations. This is consistent with ocularity invariance; binocular and monocular stimuli are judged equal in magnitude at high contrast (Baker et al., 2018; Legge, 1984; Maehara and Goryo, 2005; Meese et al., 2006).

Changing the phase relationships of stimuli under On/Off flicker had some interesting impacts on the fundamental frequency (Figure 3A). Stimuli presented in spatial phase and temporal anti-phase generated smaller SNRs ($\text{median}_{\text{SNR}} = 2.25$) than stimuli presented in spatial anti-phase and temporal phase ($\text{median}_{\text{SNR}} = 3.40$, $p = .047$). The reduction in the amplitude relative to stimuli in spatial anti-phase and temporal phase was also observed

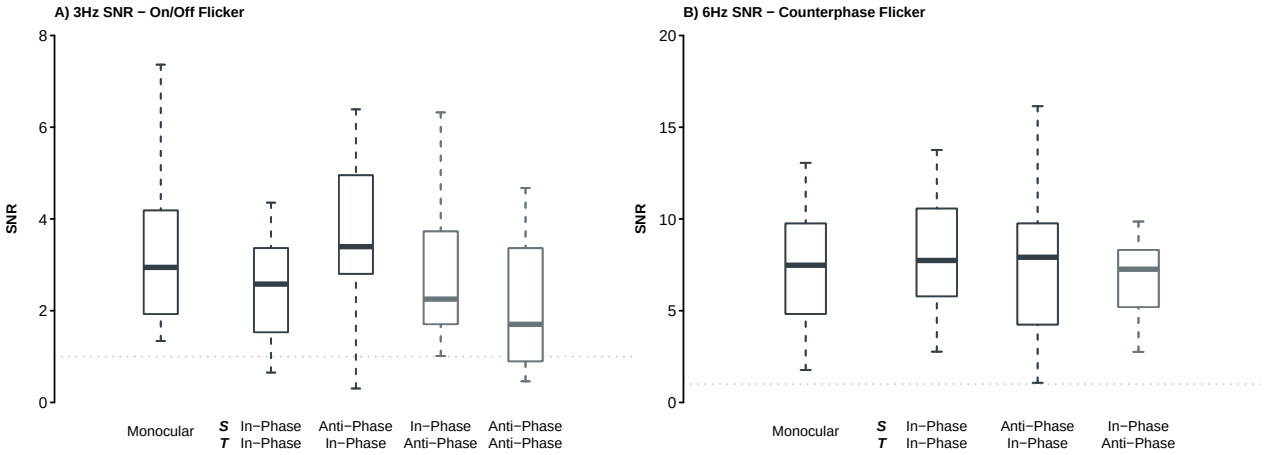

Figure 3: Boxplots of participant SNRs at the fundamental frequency for each experimental condition in our study. A) Boxplots represent the participant SNR at 3Hz. The median SNR is shown by the thick line within the box, with the lower and upper border of the box representing the first (25%) and third (75%) quartile of the SNR distribution. Dashed lines show the lower and upper whisker limits, which are calculated as 1.5 times the interquartile range (distance between the third and first quartile). Boxplots for the binocular conditions have labels for their spatial (S) and temporal (T) phase relationships. Experimental conditions where stimuli are presented in temporal anti-phase are shown in a lighter gray. B) As in A, boxplots show participant SNRs at 6Hz, the fundamental frequency for counterphase flicker. In both graphs, the dashed line represents an SNR of 1.0.

for stimuli in temporal and spatial anti-phase ($\text{median}_{\text{SNR}} = 1.70$; $p = .023$). No other statistically significant difference in median SNRs were observed for all counterphase flicker conditions or the other harmonics for On/Off flicker (all p values were greater than .05). While the median SNRs under On/Off flicker shown in temporal anti-phase were reduced in comparison to other conditions, both the spatial in phase temporal anti-phase condition ($p < .001$) and the spatial and temporal anti-phase conditions ($p = .004$) had median SNR values that were statistically significantly greater than 1.0. The presence of a 3Hz response for binocular stimuli presented in temporal anti-phase indicates that monocular responses remain and contribute to the SSVEP, as these conditions generate two transients per cycle and a purely binocular signal would only generate responses at 6Hz (Blake et al., 1981; Georgeson et al., 2016; Moulden, 1980).

Modelling

```
[1] 1.470462e+01 1.877269e+00 1.074643e+00 2.165540e+00 3.129315e-05
[6] 4.826576e+04

[1] 5.420589e+00 1.858136e+01 1.613340e+01 4.056932e-01 2.441596e-16
[6] 2.237027e-07

[1] 5.472487e+00 8.101427e+00 5.689012e+00 8.047721e-01 3.168555e-08
[6] 1.922932e+06

[1] 2.744407e+00 6.453379e+00 5.334008e-01 1.962311e-01 4.066537e-01
```

```
[6] 1.167926e+08
```

The perception of stimulus contrast across eyes is well-explained by psychophysical models that process input contrast in two sequential contrast gain control stages interposed by binocular summation (Baker et al., 2008, 2007a, 2007b; Baker and Meese, 2007; Meese et al., 2006). This simple, yet powerful, family of models not only captures behavioural data well, but can also explain neural responses to binocular and dichoptic stimuli (Baker and Wade, 2017; Lygo et al., 2021; Richard et al., 2018). Our SSVEP results show the expected pattern of binocular combination for stimuli presented at high contrast (i.e., ocularity invariance) but also intriguing effects that are likely explainable by the most recent extension of the two-stage contrast gain control model, as defined in Georgeson et al. (2016). To explore the architecture required to describe our effects adequately, we progressively increase the complexity of binocular combination beginning with a wrong model (i.e., linear combination) and building up to a multi-channel model with monocular, binocular and phase-selective pathways (Figure 4).

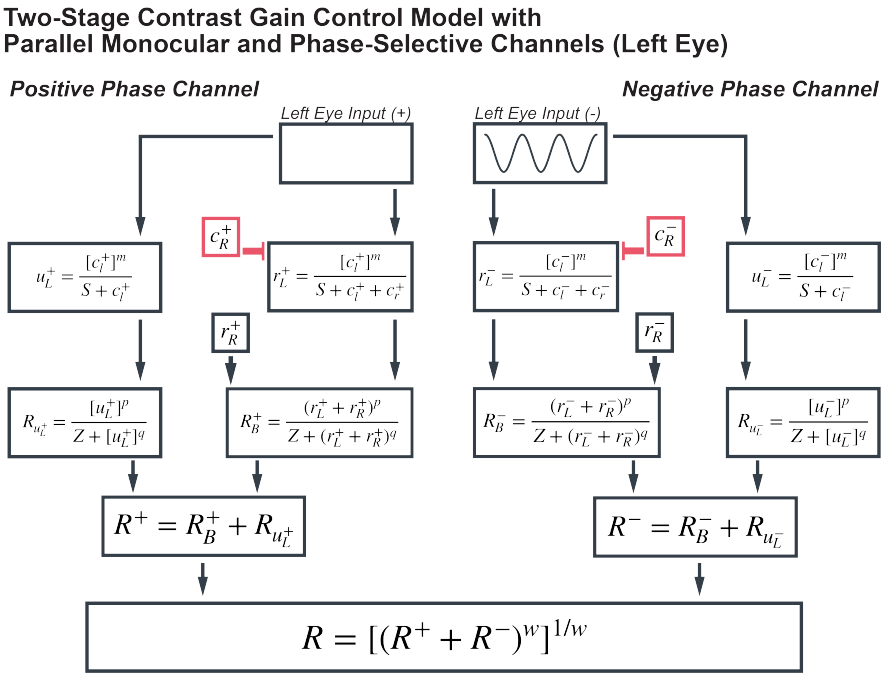

Figure 4: The multi-channel variant of the two-stage contrast gain control model. This diagram shows the channels for the left eye. Contributions from the right eye (c_R^+ and r_R^+) to the binocular channels are shown in small boxes. Unlike the model defined by Georgeson et al. (2016), responses from the parallel monocular channels are added to those of the binocular channels before signal selection for phase-selective channels. This change accounts for methodological differences when fitting neuroimaging data. To fit the final response of the model, R, was Fast Fourier Transformed, and a pink noise spectrum was added to allow for a comparable calculation of model SNRs as is done with human data.

The architecture of the models explored differs, but all received the same input and had their final outputs processed identically. The input to all models was a 3 Hz sine wave, adjusted to accurately represent the various experimental conditions of this study (see Figure 1).

For example, stimuli presented with On/Off flicker in temporal anti-phase had the left eye input generated by the following equation,

$$c_L = A * (\cos(2\pi ft) + 1)/2, \tag{4}$$

while the right eye input would be defined as,

$$c_R = A * (-\cos(2\pi ft) + 1)/2. \tag{5}$$

A represents stimulus contrast (amplitude), f the temporal flicker frequency (i.e., 3 Hz), and t time in milliseconds. The input to the other eye (c_R) is phase shifted by 180°, which can be accomplished using the negative cosine function ($-cos$). Finally, sine waves are rectified to range between 0 and 1 to represent the relative contrast presented to observers. The same experimental condition with counterphase flicker has the following sinusoidal profile for the left eye,

$$c_L = A * [\cos(2\pi ft)]_+ \tag{6}$$

and for the right eye,

$$c_R = A * [-\cos(2\pi ft)]_+. \tag{7}$$

These profiles are identical to the On/Off flicker, but the sine waves are half-wave rectified to represent the counterphase oscillation. To fit model outputs (rectified sine waves) to observer data, the final response of the models was Fast Fourier Transformed, and a pink noise spectrum was added to the Fourier amplitude, $|FFT(R_{\text{model}})| + 1/f$, before calculating model SNRs. All models developed in this study were fit by minimizing the sum of squared errors between the model output and the observer median SNRs for the first 6 SSVEP components (3Hz, 6Hz, 9Hz, 12Hz, 15Hz, and 18Hz).

Evidently wrong models

As a first step in defining the necessary architecture to capture our results, we built wrong models with no monocular stage or phase selectivity. The first is a purely linear summation model of binocular combination,

$$R_B = c_L + c_R, \tag{8}$$

the binocular response (R_B) is the sum of the monocular inputs. The fits of the linear summation model are shown in Figure 5 and its performance metrics in Table 1. For On/Off flicker, the linear summation model only generates responses at the fundamental frequency (3Hz) that grossly overestimate observer SNRs. This is expected as this model lacks the rectification and non-linearities required to generate responses at the harmonics (Regan and Regan, 1988; Wade and Baker, 2025). In a linear sum, stimuli presented under On/Off flicker in temporal anti-phase cancel each other, and thus the model generates no response. The model does generate responses at the fundamental and harmonics of the counterphase flicker condition (Figure 5B), but this is attributable to the input's rectification (the half-wave rectification applied to the input; Equation 6, Equation 7) and not the model architecture.

Model	R^2	RMSE	AIC
Linear sum	-	3.234	281.99
Linear sum, with Rectification	0.575	1.405	197.95
Two-Stage, no interocular interactions	0.822	0.908	154.86
Two-Stage, with interocular interactions	0.81	0.94	158.62
Two-Stage with parallel monocular channels	0.894	0.703	127.2
Two-Stage with phase-selective channels & monocular channels	0.899	0.684	124.28

Table 1: Goodness-of-fit metrics for all models developed in this study. Errors in predictions for the linear sum model were too large to calculate R^2. RMSE is the Root Mean Square error and AIC is the Aikaike Information Criterion.

Responses of neurons to contrast in the visual system are well-modeled by a saturating non-linearity: as contrast increases, the magnitude of responses saturates (the increase in response per unit contrast decreases at higher contrast values; Heeger (1992)). The saturating non-linearity can be modeled in different ways, but generally contains a divisive suppression and an exponentiation of the excitatory and inhibitory inputs. The inclusion of suppression can aid the model in better capturing the magnitude of responses in our observers while exponents introduces the non-linearities required to generate responses at the harmonic frequencies. Thus, the next increment in our model complexity defines the binocular response as the contrast gain control equation

$$R_B = \frac{(c_L + c_R)^p}{Z + (c_L + c_R)^q}, \tag{9}$$

where the binocular response of the model (R_B) is defined as the sum of monocular inputs (c_L and c_R) raised to the power p normalized by the sum of monocular inputs raised to the power q and where ($p > q$). The parameter Z prevents division by zero. The model can now generate responses at the harmonic frequencies for stimuli presented in temporal phase under On/Off flicker (see Figure 5 and Table 1). While this model iteration improves on the fits, it nevertheless struggles to fit SNR values at the fundamental frequency (3Hz) and is, as with the linear summation model, incapable of generating responses to stimuli presented with On/Off flicker in temporal anti-phase; the linear sum of stimuli presented in temporal anti-phase will always return zero. The model, therefore, still lacks the necessary architecture to adequately define neural responses to our stimuli.

The Two-Stage Contrast Gain Control Model

The simple models described above could not accurately represent the observer SSVEPs we recorded. They overestimated SNRs at the fundamental frequency and failed to generate responses for stimuli presented in temporal anti-phase with On/Off flicker. A potential refinement to the model is add a monocular transducer prior to binocular combination Baker

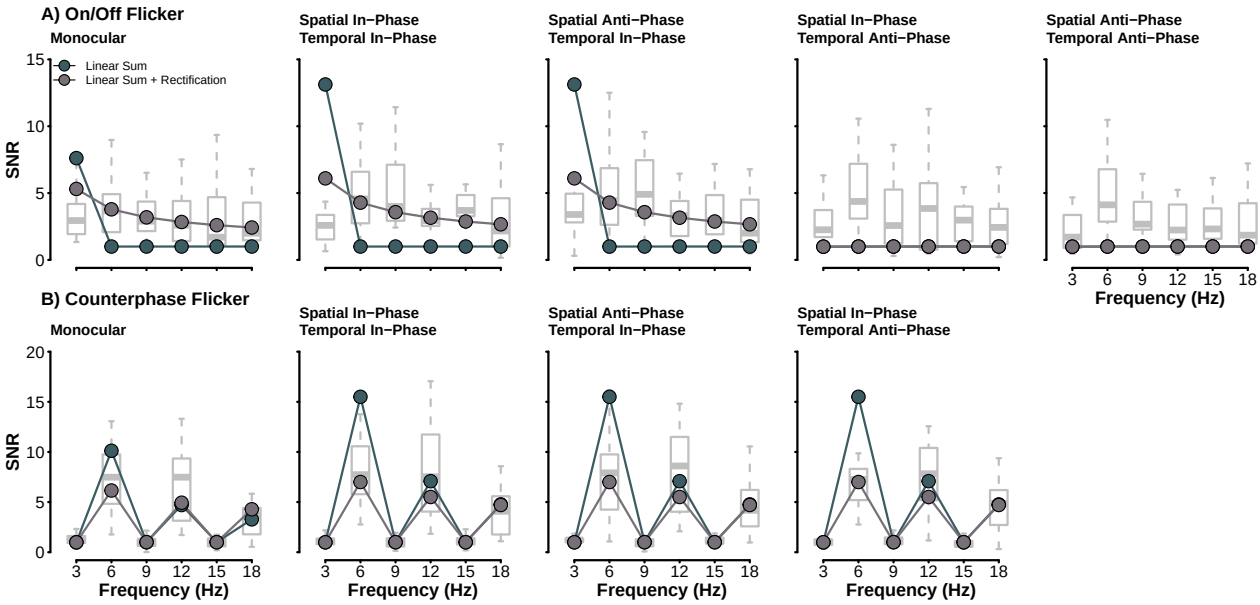

Figure 5: Fits of the linear sum (green) and the rectified linear sum (brown) models. Boxplots behind model responses show the distribution of observer SNRs. Model SNRs were fit to the median SNR of observers, which is represented by the thicker line within the box.

et al. (2018). The architecture of this model now begins with a monocular stage

$$r_L = \frac{c_L^m}{S + c_L}, \qquad r_R = \frac{c_R^m}{S + c_R} \tag{10}$$

where a non-linearity (m) is applied to the monocular inputs (c_L and c_R) in addition to self-suppression. The outputs of the monocular stage are then fed into a binocular stage that undergoes a second contrast gain control,

$$R_B = \frac{(r_L + r_R)^p}{Z + (r_L + r_R)^q}. \tag{11}$$

In this model variant, m is the monocular excitatory component and determines the extent of summation at detection threshold, moderated by the suppressive term. In the second stage, $p > q$ as with Equation 9, which is necessary to capture the facilitative effects of dichoptic masking (Meese et al., 2006). We can strengthen the normalization of the monocular input by adding interocular suppression and replacing Equation 10 (the first stage) with

$$r_L = \frac{c_L^m}{S + c_L + c_R}, \qquad r_R = \frac{c_R^m}{S + c_R + c_L}. \tag{12}$$

This model iteration is identical to the two-stage contrast gain control model defined by Meese et al. (2006).

The fits of both model variants, with and without interocular suppression, are shown in Figure 6. The difference in their quality is negligible (see Table 1) as both fit most experimental conditions well. The addition of the monocular transducer enables the model

to fit observer SNRs at the fundamental frequency for stimuli presented in temporal phase under On/Off flicker and importantly, it now generates responses for stimuli presented in temporal anti-phase. The transduced monocular inputs no longer cancel each other at the binocular stage. While the model can generate responses to temporal anti-phase stimuli, it only does so at the even-harmonics (2F-6Hz, 4F-12Hz, and 6F-18Hz) of the SSVEP spectrum. This is to be expected as the model can only generate binocular responses; it does not preserve monocular responses beyond the first stage. As the two rectified sine waves are in anti-phase, their sum will generate a new waveform with frequencies at twice the frequency of the original (6Hz) and its integer harmonics (2F-12Hz and 3F-18Hz; see Figure 8 **maybe in the appendix?**). The responses at the fundamental frequency (3Hz) and its odd integer harmonics (3F - 9Hz, 5F - 15Hz) of our observers cannot be explained by an architecture with a purely binocular output. Next we explore how the addition of parallel monocular channels may aid in explaining observer responses to stimuli presented in temporal anti-phase.

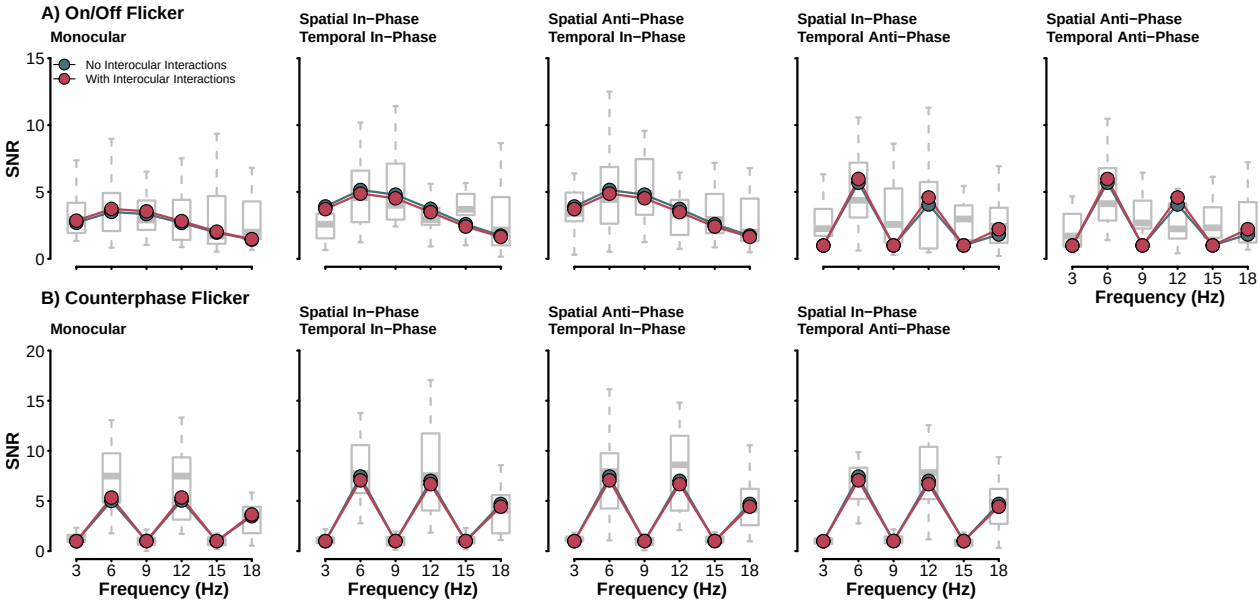

Figure 6: Fits of the two-stage contrast gain control model without (green) and with (red) interocular suppression. Boxplots behind model responses show the distribution of observer SNRs. Model SNRs were fit to the median SNR of observers, which is represented by the thicker line within the box.

Parallel Monocular and Phase-Selective Channels

To preserve the monocular responses until the output of the model, we add parallel monocular channels as was suggested by Georgeson et al. (2016). These channels are fully monocular and therefore have no interocular suppression term,

$$\mu_L = \frac{C_L^m}{S + C_L}, \qquad \mu_R = \frac{C_R^m}{S + C_R}, \tag{13}$$

where μ_L is the output of the first stage of the monocular channel for the left eye, and μ_R is that of the right eye. The excitatory exponent m is identical to that in the channels that

include binocular interaction (Equation 12). The output of the monocular channel undergoes a second rectification and normalization, identical to that of the binocular channel,

$$R_{\mu_L} = \frac{\mu_L^p}{Z + \mu_L^q}, \qquad R_{\mu_R} = \frac{\mu_R^p}{Z + \mu_R^q}, \tag{14}$$

where R_{μ_L} and R_{μ_R} represent the final responses of the left and right monocular channels. The parameters m, p, q, S and Z are identical to those of the binocular channel and thus no additional free parameters are required to define the parallel monocular channels. The addition of these channels poses an interesting problem regarding cue selection. The final stage of this model has three channel responses: monocular left (R_L), monocular right (R_R), and binocular (R_B). In behavioural variants of this model (Georgeson et al., 2016), cue selection is implemented as a MAX rule, as a Minkowski sum with a very large ($\approx$ 30) exponent. This method of signal combination was not appropriate for our data, because in SSVEP paradigms the recorded signal measured at the scalp is the pooled activity of all responsive neurons. In the model, the binocular response is always larger than the monocular response and thus dominates in the final signal, preventing a model with MAX pooling from capturing the fundamental and odd-harmonics responses for anti-phase stimuli. Instead, we found that a linear combination of the binocular signal and the monocular signals,

$$R = R_B + R_{\mu_L} + R_{\mu_R}, \tag{15}$$

generated better fits to our data. In our model fits, we use the monocular response from the left eye (R_{μ_L}) to add to the binocular channel. [Not sure I understand this bit - why not add both monocular channels?] Adding parallel monocular channels to the two-stage contrast gain control model significantly improved the fit of our observer data (Figure 7). With the monocular response preserved, the model can now generate SSVEPs at the fundamental frequency and odd-harmonics necessary to capture observer data for stimuli presented in temporal anti-phase under On/Off flicker (see Table 1). Thus, monocular responses to binocular stimuli are preserved along the processing pipeline and can be recorded in the SSVEPs of observers.

Our results do not show a strong effect of stimulus spatial phase on observer SSVEPs. Still, it is important to determine whether adding phase-selective channels to the two-stage contrast gain control model highlights a subtle impact of phase-selective responses. We add phase-selective channels to the binocular and monocular channels of the two-stage contrast gain control model. Phase-selectivity required replicating the equations from both stages to have binocular and monocular channels selective for either positive or negative phase (see Figure 4). The phase-selective channels in this model are completely independent; they do not interact with each other. This model iteration, which we refer to as the full model, replicates the two-stage contrast gain control model developed by Georgeson et al. (2016).

As we encountered above with the addition of monocular channels, the addition of phase-selectivity means that we now have two final signals following the combination of the binocular and monocular channels (Equation 15), a positive phase and a negative phase signal. To generate the final model SSVEP, we use a MAX rule implemented as a Minkowski sum, as was done in Georgeson et al. (2016),

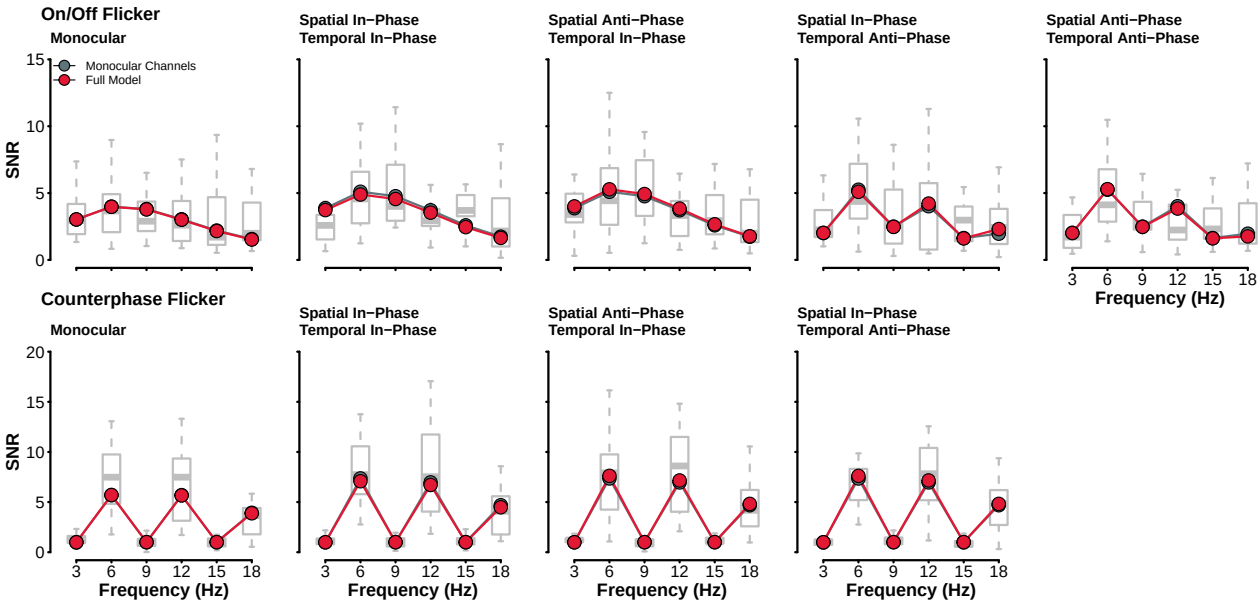

Figure 7: Fits of the two best performing models to our observer data. Both models, that including parallel monocular channels and the full model with the added phase-selective channels perform quite similarly. The two stage contrast gain control model with parallel monocular channels is sufficient to explain the effects in our data. The best fitting parameters for the monocular channels model were: m = 2.68, p = 8.72, q = 2.03, S = 0.25, Z = -0.02. These parameters suggest strong binocular combination at the monocular stage.

$$R_{\text{MAX}} = [(R^{+})^{w} + (R^{-})^{w}]^{\frac{1}{w}}. \tag{16}$$

We introduce the new parameter w, which is expected to be large (> 20) to select the phase channel, either positive or negative, that generated the largest response. The addition of phase-selectivity to our model improved the fits slightly as the overall R^2 was increased. The Aikaike Information Criterion (AIC) of the phase selective model (AIC = 124.28) is slightly smaller than that of the two-stage contrast gain control model with parallel monocular channels (AIC = 127.2). While the effects of spatial phase on observer SSVEPs are small, accounting for its impact on our model by adding phase-selective channels offers a better description of our results.

While the whole model outperformed the others, the simpler models are nested variants and thus difficult to compare using R^2 and AIC values alone. We use an F test for nested models to determine if the difference in the quality of fits between our smaller models and the full model is statistically significant. The full results of the F tests are reported in **?@tbl-fTable**. We do not find a statistically significant difference between the fits of the two-stage contrast gain control with parallel monocular channels and the full model, $F(1, 47) = 4.00, p = .051$. While the full model does improve model fits, its contributions to explaining our findings are not sufficiently large to pass the F test for nested models, at an α level of .05.

Parameter	Value
m	5.47
p	8.1
q	5.69
S	0.8
Z	0

Discussion

References

Bacon, J.H., 1976. The interaction of dichoptically presented spatial gratings. Vision Res 16, 337–44. https://doi.org/10.1016/0042-6989(76)90193-0

Baker, D.H., Lygo, F.A., Meese, T.S., Georgeson, M.A., 2018. Binocular summation revisited: Beyond $\sqrt{2}$. Psychol Bull 144, 1186–1199. https://doi.org/10.1037/bul0000163

Baker, D.H., Meese, T.S., 2007. Binocular contrast interactions: Dichoptic masking is not a single process. Vision Res 47, 3096–107. https://doi.org/10.1016/j.visres.2007.08.013

Baker, D.H., Meese, T.S., Georgeson, M.A., 2007a. Binocular interaction: Contrast matching and contrast discrimination are predicted by the same model. Spat Vis 20, 397–413. https://doi.org/10.1163/156856807781503622

Baker, D.H., Meese, T.S., Hess, R.F., 2008. Contrast masking in strabismic amblyopia: Attenuation, noise, interocular suppression and binocular summation. Vision Res 48, 1625–40. https://doi.org/10.1016/j.visres.2008.04.017

Baker, D.H., Meese, T.S., Summers, R.J., 2007b. Psychophysical evidence for two routes to suppression before binocular summation of signals in human vision. Neuroscience 146, 435–448. https://doi.org/10.1016/j.neuroscience.2007.01.030

Baker, D.H., Wade, A.R., 2017. Evidence for an optimal algorithm underlying signal combination in human visual cortex. Cereb Cortex 27, 254–264. https://doi.org/10.1093/cercor/bhw395

Blake, R., 1989. A neural theory of binocular rivalry. Psychol Rev 96, 145–67. https://doi.org/10.1037/0033-295x.96.1.145

Blake, R., Overton, R., Lema-Stern, S., 1981. Interocular transfer of visual aftereffects. J Exp Psychol Hum Percept Perform 7, 367–81. https://doi.org/10.1037//0096-1523.7.2.367

Blake, R., Wilson, H., 2011. Binocular vision. Vision Research 51, 754–770. https://doi.org/10.1016/j.visres.2010.10.009

Campbell, F.W., Green, D.G., 1965. Monocular versus binocular visual acuity. Nature 208, 191–2. https://doi.org/10.1038/208191a0

Chatrian, G.E., Lettich, E., Nelson, P.L., 1985. Ten percent electrode system for topographic studies of spontaneous and evoked EEG activities. American Journal of EEG Technology 25, 83–92. https://doi.org/10.1080/00029238.1985.11080163

Delorme, A., Makeig, S., 2004. EEGLAB: An open source toolbox for analysis of single-trial EEG dynamics including independent component analysis. Journal of Neuroscience Methods 134, 9–21. https://doi.org/10.1016/J.JNEUMETH.2003.10.009

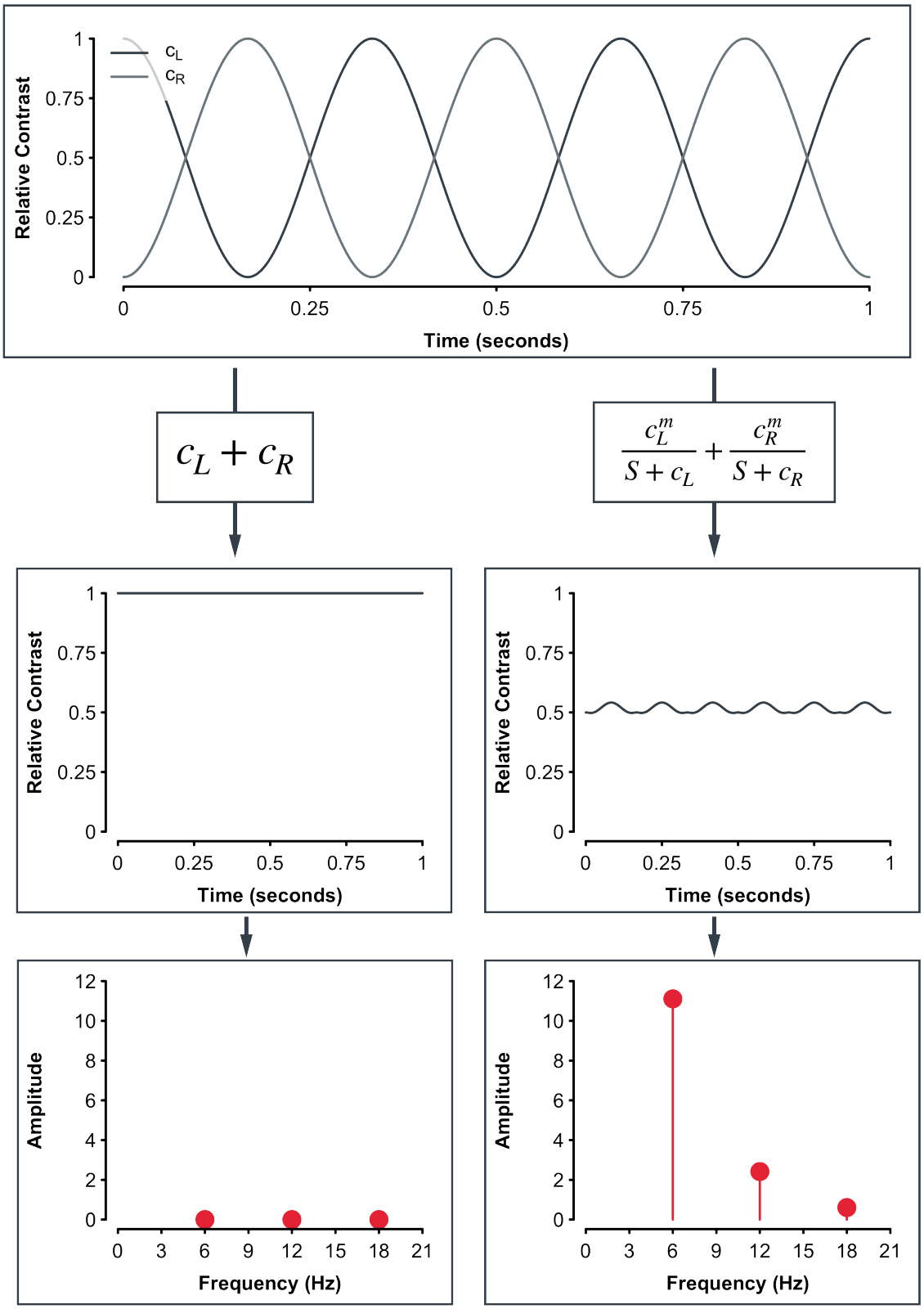

Figure 8: A diagram that shows the effect of summing a rectified wave.

Ding, J., Klein, S.A., Levi, D.M., 2013. Binocular combination of phase and contrast explained by a gain-control and gain-enhancement model. J Vis 13, 13. https://doi.org/10.1167/13.2.13

Ding, J., Sperling, G., 2006. A gain-control theory of binocular combination. Proc Natl Acad Sci U S A 103, 1141–6. https://doi.org/10.1073/pnas.0509629103

Georgeson, M.A., Wallis, S.A., Meese, T.S., Baker, D.H., 2016. Contrast and lustre: A model that accounts for eleven different forms of contrast discrimination in binocular vision. Vision Research 129, 98–118. https://doi.org/10.1016/j.visres.2016.08.001

Hansen, B.C., Hess, R.F., 2006. Discrimination of amplitude spectrum slope in the fovea and parafovea and the local amplitude distributions of natural scene imagery. J Vis 6, 696–711. https://doi.org/10.1167/6.7.3

Heeger, D.J., 1992. Normalization of cell responses in cat striate cortex. Vis Neurosci 9, 181–97. https://doi.org/10.1017/s0952523800009640

Legge, G.E., 1984. Binocular contrast summation–i. Detection and discrimination. Vision Res 24, 373–83. https://doi.org/10.1016/0042-6989(84)90063-4

Lygo, F.A., Richard, B., Wade, A.R., Morland, A.B., Baker, D.H., 2021. Neural markers of suppression in impaired binocular vision. Neuroimage 230, 117780. https://doi.org/10.1016/j.neuroimage.2021.117780

Maehara, G., Goryo, K., 2005. Binocular, monocular and dichoptic pattern masking. Optical Review 12, 76–82. https://doi.org/DOI 10.1007/s10043-004-0076-5

Meese, T.S., Baker, D.H., 2011. Contrast summation across eyes and space is revealed along the entire dipper function by a "swiss cheese" stimulus. J Vis 11, 1–23. https://doi.org/10.1167/11.1.23

Meese, T.S., Georgeson, M.A., Baker, D.H., 2006. Binocular contrast vision at and above threshold. Journal of vision 6, 1224–1243. https://doi.org/10.1167/6.11.7

Moradi, F., Heeger, D.J., 2009. Inter-ocular contrast normalization in human visual cortex. J Vis 9, 13 1–22. https://doi.org/10.1167/9.3.13

Moulden, B., 1980. After-effects and the integration of patterns of neural activity within a channel. Philos Trans R Soc Lond B Biol Sci 290, 39–55. https://doi.org/10.1098/rstb.1980.0081

Regan, M., Regan, D., 1988. A frequency domain technique for characterizing nonlinearities in biological systems. Journal of theoretical biology 133, 293–317.

Richard, B., Chadnova, E., Baker, D.H., 2018. Binocular vision adaptively suppresses delayed monocular signals. Neuroimage 172, 753–765. https://doi.org/10.1016/j.neuroimage.2018.02.021

Simmons, D.R., 2005. The binocular combination of chromatic contrast. Perception 34, 1035–1042. https://doi.org/10.1068/p5279

Simmons, D.R., Kingdom, F.A.A., 1998. On the binocular summation of chromatic contrast. Vision Research 38, 1063–1071. https://doi.org/10.1016/S0042-6989(97)00272-1

Tadmor, Y., Tolhurst, D.J., 1994. Discrimination of changes in the second-order statistics of natural and synthetic images. Vision Research 34, 541–554. https://doi.org/10.1016/0042-6989(94)90167-8

Wade, A.R., Baker, D.H., 2025. Measuring contrast processing in the visual system using the steady state visually evoked potential (SSVEP). Vision Research 231, 108614. https://doi.org/10.1016/j.visres.2025.108614

Wilson, H.R., 2003. Computational evidence for a rivalry hierarchy in vision. Proceedings of the National Academy of Sciences of the United States of America 100, 14499–14503. https://doi.org/10.1073/pnas.2333622100